Phase Behavior and Dielectric Spectroscopy of the Sodium Dodecyl Trioxyethylene Sulfate/*n*-Butanol/Water System

WEI, Su-Xiang[c] (魏素香) MU, Jian-Hai[a] (牟建海) ZHAO, Kong-Shuang[*,b] (赵孔双)
LEI, Jian-Ping[c] (雷建平) LI, Gan-Zuo[a] (李干佐)

[a] *Key Laboratory for Colloid & Interface Chemistry of State Education Ministry, Shandong University, Jinan, Shandong 250100, China*

[b] *Department of Chemistry, Beijing Normal University, Beijing 100875, China*

[c] *Department of Chemistry, South China Normal University, Guangzhou, Guangdong 510631, China*

The phase diagram of the ternary system of sodium dodecyl trioxyethylene sulfate (SDES)/*n*-butanol/water is obtained at (30.0 ± 0.1) ℃. There exists a clear, isotropic, and low-viscosity L phase, which could be divided into W/O micelle, bicontinuous (B.C.) phase and O/W micelle by conductivity measurements. Dielectric Relaxation Spectroscopy (DRS) measurements are applied to investigate microstructure changes of this system. For samples with a fixed weight ratio, SDES/*n*-butanol = 3/7, DRS indicates a structure transition from W/O to O/W micelles via B.C. phase with the increase of water content. For the samples with a fixed weight ratio, SDES/H_2O = 4/6, DRS can presents that there exist changes of onefold structure size of W/O micelles as *n*-butanol content increases. The results obtained from DRS and their analyses are in good agreement with those from phase diagram and conductivity measurements.

Keywords phase behavior, conductivity, dielectric relaxation spectroscopy, micelle

Introduction

It is well known that surfactants in an aqueous solution could form micelles at a concentration higher than the critical micelle concentration (cmc). Knowledge of alcohol solubilization in aqueous micelle solutions is important in understanding the aggregation behavior of such systems and is relevant to several industrial processes.[1] Many studies have been reported on phase behavior of ternary systems of ionic surfactant, alcohol, and water.[2-7] Generally, in the case of short chain alcohol, a transparent, isotropic, and low-viscosity phase appears extending from the water corner to the alcohol corner, which is called L phase. This region divides into two subregions, L_1 and L_2, namely normal micelles and reverse micelles. Conductivity measurements can determine different microstructures in L phase of an ionic surfactant system.

Dielectric Relaxation Spectroscopy (DRS) is a noninvasive and rapid method for the structural characterization and quality control of materials, because it only needs a small a.c. voltage and it is very sensitive to molecular motion and structure.[8] DRS is an effective tool to probe the physicochemical properties and inner structure of a system. It has been successfully used to determine the structural, dynamic, and electric properties of some molecular organized assembles.[9,10] Many reports have been focused on dielectric relaxation behavior of such systems in high frequency range 10^6—10^{11} Hz.[11-15] A few researchers have primarily investigated that in low frequency range.[16,17]

In this paper, the ternary phase diagram of sodium dodecyl trioxyethylene sulfate (SDES)/*n*-butanol/water is obtained and phase behavior is discussed. DRS in low frequency range from 5 to 10^5 Hz is applied to examine structure transition when one component content of the system varies, and it is in good agreement with the results obtained from phase diagram and conductivity measurements.

Experimental

Materials

Anionic surfactant, sodium dodecyl trioxyethylene sulfate (SDES), with the formula $CH_3(CH_2)_{11}(OCH_2CH_2)_3OSO_3Na$, purchased from Henkel Ltd. (Germany), was recrystallized three times from ethanol and characterized by the melting point (148—150 ℃) and cmc (2.5×10^{-3} mol/L, no minimum point). *n*-Butanol was of analytical reagent grade. All samples were prepared with deionized water.

* E-mail: zhaoks@bnu.edu.cn

Received December 27, 2002; revised May 22, 2003; accepted June 18, 2003.

Project supported by the Visiting Scholar Foundation of Key Laboratory in Chinese University, the National Natural Science Foundation of China (No. 20273010 and 29873015), the Natural Science Foundation of Guangdong Province and the Basic Study Project of Guangzhou City.

Phase diagram

Samples for phase diagram were prepared by weighing the desired amount of SDES and n-C_4H_9OH with a varying weight ratio from 0∶10 to 10∶0. Deionized water was added to the samples gradually while stirring at (30.0 ± 0.1) ℃. The isotropic uniphasic region (L phase) of the phase behavior was determined by visual observation and conductivity measurements, and the liquid crystalline region was not studied in this paper.

Conductivity measurements

Conductivity measurements were performed with a conductometer (Model DDS—11A, Shanghai Instrument Ltd., China) and a glass electrode, calibrated with a 10 mmol/L KCl solution. The SDES/n-C_4H_9OH solution was put in a thermostated bottle and the required water was added. All measurements were done at (30.0 ± 0.1) ℃. To guarantee homogeneity of the solution, it was stirred for 10 min and then placed for a while before the measurements of electrical conductivity and dielectric spectroscopy were carried out.

Dielectric measurements

Dielectric measurements were carried out at (30.0 ± 0.1) ℃ by HP 4192A LF Impedance analyzer made by Hewlett Packard Co. Ltd. The measuring cell consists of two concentric platinum cylinderal electrodes fixed at the bottom of a glass vessel. The applied voltage in all measurements was 5 mV, and dielectric response was measured in the frequency range from 5 to 10^5 Hz. Data were collected in the form of parallel connection of capacitance (C) and conductance (G) as functions of frequency. Many checks and repeated measurements have been made throughout the process to ensure that the data were reproducible.

Results and discussion

Phase behavior

Fig. 1 shows the L phase of the phase diagram of SDES/n-C_4H_9OH/H_2O system determined over the whole concentration range at (30.0 ± 0.1) ℃. The L phase is a clear, isotropic, and low-viscosity phase that extends from the water corner to the alcohol corner.

In order to determine different structures in L phase, conductivity of samples with different surfactant (wt%)/alcohol (wt%) ratios versus water concentration is shown in Fig. 2. The conductivity values describe an approximate parabola against water concentration, which increase dramatically at low water content, and then increase slowly to a maximum, finally decrease at higher water content. The shape of conductivity curves could correspond to the transition from reverse micelles (W/O) to normal micelles

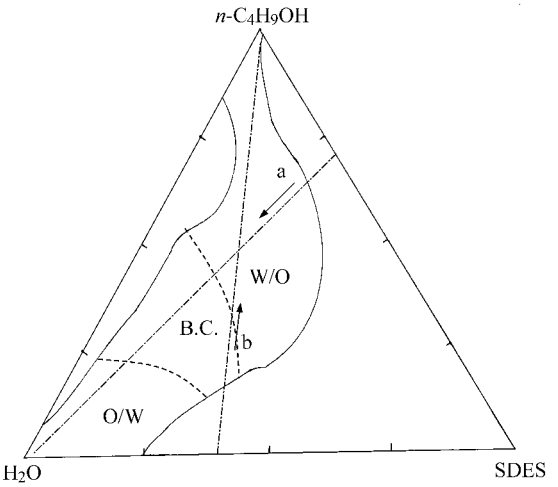

Fig. 1 L phase region of the three-component phase diagram for the SDES/n-C_4H_9OH/H_2O system at (30.0 ± 0.1) ℃.

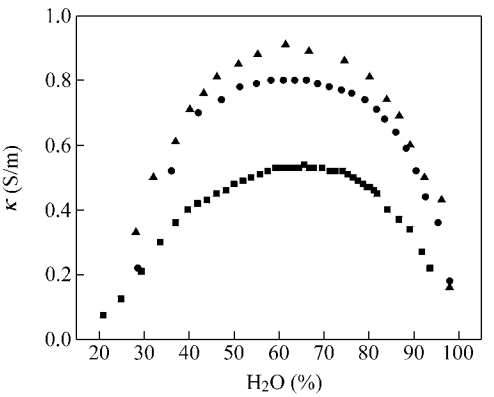

Fig. 2 Conductivity versus water content at different SDES (wt%)/n-C_4H_9OH (wt%) ratios: ■, 2:8, ●, 4:6 and ▲, 5:5.

(O/W) via a transition state that may be bi-continuous phase (B.C.), which is similar to that of microemulsions, but not the same as most of surfactant/alcohol/water systems that only form reverse micelles and mixed micelles.[5-7] In reverse micelle region, solubilization of water in the palisade layer and inner core of micelles leads to an increase in the size of micelle and surfactant ionization, resulting in a rapid increase of conductivity. However, in bicontinuous phase with water content range from about 40% to 60%, the addition of water cannot make microstructure evidently change because of the special pipeline structure, so that conductivity almost shows less dependence on water content. The decrease in conductivity with water concentration increasing in a high water content region agrees with O/W micelle formation in an aqueous solution. The amount of surfactant and alcohol decreases at the same time as the water content increases and conductivity becomes smaller. Besides the incorporation of alcohol in SDES, micelles produce surfactant ionization, which also agrees with the decrease in conductivity with the water content. In addition, it also can be seen from Fig. 2 that conductivity is larger in solution with a higher surfactant

(wt%)/alcohol (wt%) ratio, and it also can be explained from the viewpoint of surfactant ionization. The increase in SDES concentration enhances ionic strength of samples, and conductivity increases correspondingly.

Dielectric relaxation spectroscopy

According to the phase behavior of SDES/*n*-C_4H_9OH/H_2O system, two groups of samples were investigated by dielectric relaxation spectroscopy (DRS) method: (i) water was added gradually (15.7%—95.0%) to the solution at a fixed SDES (wt%)/*n*-C_4H_9OH (wt%) ratio of 3:7, and (ii) alcohol was added gradually (39.6%—80.0%) to the solution at a fixed SDES (wt%)/H_2O (wt%) ratio of 4:6, which have been labeled as segments a and b in Fig. 1 respectively. As can be seen from Fig. 2, the dc conductivity can determine the microstructure of micelle. Compared to the dc conductivity, the DRS can also give structural information of systems measured, of which two main parameters are permittivity and ac conductivity. In this paper, the DRS method was adopted to further validate the structural properties of micellar systems.

Varying the water content

Permittivity (ε) and conductivity (κ) are shown in Fig. 3 (a) and (b) as functions of frequency for samples with different water content. It is obvious that there exists a remarkable dielectric relaxation phenomenon over the frequency range measured, which results from the structure of heterogeneous system, because of phase interface between disperse phase and medium. The conductivity of the systems changes regularly at high frequency range, and the change extent is different for the different water contents. The increment in conductivity with water content is so called dielectric relaxation or conductivity relaxation. Dielectric relaxation can be caused by interfacial polarization.[18] The steep rise in permittivity at frequency lower than 20 Hz is attributed to electrode polarization, which is not the characteristic of specimen. Additionally, permittivity in Fig. 3(a) is abnormally large. It is possible that electrode polarization still contributes to the values of permittivity in the frequency range of 20—10^4 Hz, which results in the value of apparent permittivity deviating from real value. In order to get rid of the effect of electrode polarization, raw dada are corrected as follows.[19]

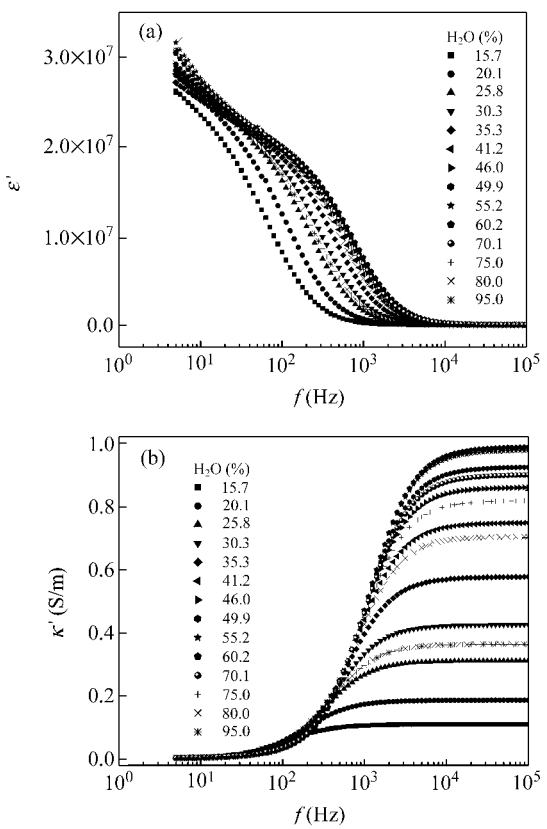

Fig. 3 Permittivity (a) and conductivity (b) as functions of frequency for the systems with different water content.

$$C_s = \frac{C_x(1+\omega^2 L_r C_x) + L_r G_x^2}{(1+\omega^2 L_r C_x)^2 + (\omega L_r G_x)^2} - C_f \quad (1)$$

$$G_s = \frac{G_x}{(1+\omega^2 L_r C_x)^2 + (\omega L_r G_x)^2} \quad (2)$$

where C_s and G_s represent real capacitance and cooductance of the samples, namely data corrected, respectively. C_x and G_x denote capacitance and conductance measured, respectively. L_r and C_f are coefficients of inductance and pelagic capacitance, respectively. C_s and G_s were used for further calculation and analyses. It also can be seen from Fig. 3 that f_0 [characteristic relaxation frequency: frequency when relaxation strength is equal to $(\varepsilon_l - \varepsilon_h)/2$] shifts to high frequency side for permittivity and relaxation intensions increase for conductivity with water content at first, and then turn to the low side and decrease respectively when water content is larger than 60.2% in the frequency range 20—10^4 Hz. This relaxation behavior reflects microstructure transition of system as discussed in Fig. 1 and Fig. 2.

In order to obtain more detailed information about systems, dielectric parameter group (ε_l: low-frequency permittivity; ε_h: high-frequency permittivity; f_0; κ_l: low-frequency conductivity; κ_h: high-frequency conductivity) was accurately got by non-linear curve fitting for experimental curves. Fig. 4 gives an example about fitting at the water content of 55.2%. Over lower frequency range the steep increase in permittivity caused by electrode polarization is not discussed in present paper. During the fitting process, Cole-Cole formulae as below were used,[20] where ω ($=2\pi f$) and τ_0 ($=1/2\pi f_0$) are angular frequency and characteristic relaxation time respectively, and the parameter α are the values between 0 and 1, the former value giving the result of Debye model for polar dielectrics.

$$\varepsilon = \varepsilon_h + \frac{(\varepsilon_l - \varepsilon_h)[1 + (\omega\tau_0)^{1-\alpha}\sin(\pi\alpha/2)]}{1 + 2(\omega\tau_0)^{1-\alpha}\sin(\pi\alpha/2) + (\omega\tau_0)^{2(1-\alpha)}} \quad (3)$$

$$\kappa = \kappa_l + \frac{(\varepsilon_l - \varepsilon_h)\omega\varepsilon_0(\omega\tau_0)^{1-\alpha}\cos(\pi\alpha/2)}{1 + 2(\omega\tau_0)^{1-\alpha}\sin(\pi\alpha/2) + (\omega\tau_0)^{2(1-\alpha)}} \quad (4)$$

The above five dielectric parameters for the samples with different water content obtained by fitting the experimental curves in Fig. 3, are listed in Table 1.

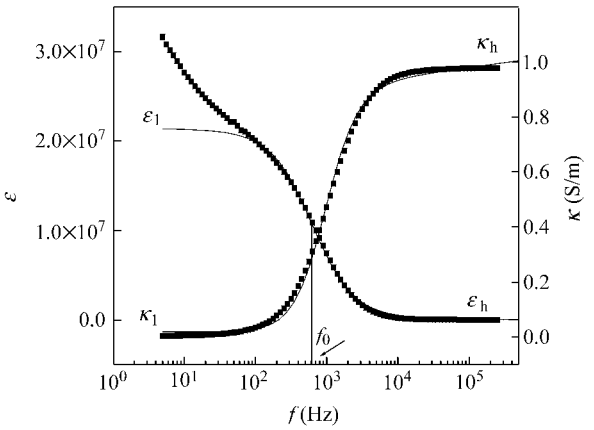

Fig. 4 An example of the fitting for experimental lines.

Table 1 Dielectric parameters obtained by fitting the experimental curves in Fig. 3

H_2O (%)	$10^{-7}\varepsilon_l$	$10^{-4}\varepsilon_h$	f_0 (Hz)	$10^2\kappa_l$ (S/m)	κ_h (S/m)
15.70	2.40	0.94	61.80	0.62	0.11
20.10	2.38	1.02	105.39	0.65	0.18
25.80	2.30	1.09	183.54	0.73	0.31
30.30	2.25	1.13	258.28	0.83	0.42
35.30	2.19	1.22	363.03	0.87	0.57
41.20	2.16	1.26	478.07	0.92	0.75
46.00	2.15	1.28	548.86	1.00	0.86
49.90	2.14	1.26	590.46	1.06	0.92
55.20	2.14	1.26	621.83	1.34	0.97
60.20	2.14	1.22	623.27	1.43	0.99
70.10	2.16	1.18	558.65	1.32	0.90
75.00	2.19	1.12	492.74	1.21	0.82
80.00	2.25	1.03	405.92	1.09	0.70
95.00	2.32	0.98	206.11	0.92	0.36

According to these dielectric parameter values, relaxation strength, $\Delta\varepsilon$ $(=\varepsilon_l - \varepsilon_h)$ and $\Delta\kappa$ $(=\kappa_h - \kappa_l)$ and characteristic relaxation time τ_0 were obtained as functions of water content, which are presented in Fig. 5 and Fig. 6.

As can be seen in Fig. 5, there exist three regions in both curves. When the water content is smaller than 40%, relaxation strength, $\Delta\varepsilon$ or $\Delta\kappa$, decreases or increases dramatically. Then the changes become slower and slower in the range of water content from 40% to 60%. Finally, $\Delta\varepsilon$ increases and $\Delta\kappa$ decreases at higher water content. In other words, there are two inflexions for the changes of relaxation strength with water content, one at about 40% and the other at about 60%, which is in better accordance with the structure transition point shown in Fig. 1 and Fig. 2. The fact further indicates that DRS is the macro-exhibition of the microstructure of systems.

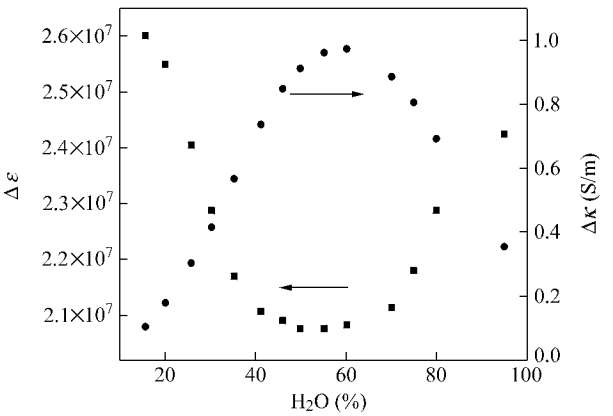

Fig. 5 Relaxation strength, $\Delta\varepsilon$ (■) and $\Delta\kappa$ (●) as functions of water content.

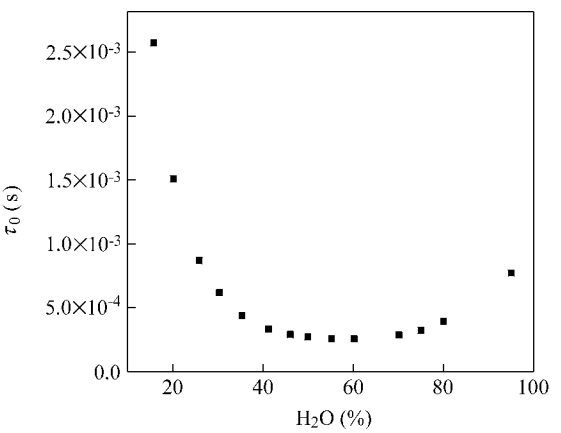

Fig. 6 Characteristic relaxation time τ_0 as a function of water content.

The pure electrode polarization phenomenon on permittivity and conductivity is that relaxation strength increases and decreases respectively and characteristic relaxation frequency shifts to low frequency range with water content for an electrolyte solution. From Fig. 5 and Fig. 6, it can be seen that the relaxation strength and f_0 exhibit inflexions with water content. So it could be said that relaxations in Fig. 3 (a) are the reflection of inner structural changes of the system, but not pure electrode polarization phenomenon. It is estimated that the dielectric relaxation is just affected by electrode polarization, exhibiting in value of permittivity.

Another important dielectric parameter, macroscopic characteristic relaxation time τ_0 that reflects the mean polarization velocity, is a dynamic parameter. Fig. 6 shows that τ_0 has an analogous trend with the strength of permittivity $(\Delta\varepsilon)$ when the water content increases: τ_0 decreases rapidly and then changes slowly and finally increases with water content. Two inflexions are seen at about 40% and 60% water content, too. It is very interesting to find that

τ_0 also relates to aggregate structure of systems studied.

There is a little water in W/O micelles, which restricts the movement of ions, resulting in a slower relaxation process and a longer relaxation time (generally larger than 1 ms). The increase in water content expedites the transfer velocity of ions, making conductivity of the system increase and τ_0 decrease gradually. In B.C. phase, because of the existence of the special pipeline structure, the movement of ions is free and the relaxation process is fast. Furthermore, there is little effect of the increase of water content on the special structure, so τ_0 is short in B.C. phase (generally less than 0.5 ms), and because of the existence of the special pipeline structure, the movement of ions will be more free compared with that in W/O or O/W regions and the relaxation process is fast. However, in O/W micelle region, the existence of large amount of water also speeds up the movement of ions, leading to a faster relaxation process compared with that in W/O micelles. On the other hand, the concentration of ions and micelles decreases with the increase of water content, resulting in a decrease in polarization velocity of particles; therefore, τ_0 becomes longer (larger than 0.5 ms).

It should be reasonable to suppose that the present system is a concentrated dispersion of spherical particles, so phase parameters (φ: volume fraction; κ_i, κ_a: inner and outer phase conductivity) were further obtained by Hanai formula:[21]

$$\frac{\varepsilon^* - \varepsilon_i^*}{\varepsilon_a^* - \varepsilon_i^*}\left(\frac{\varepsilon_a^*}{\varepsilon^*}\right)^{1/3} = 1 - \phi \qquad (5)$$

where ε^* is complex permittivity for the whole system, ε_i^* and ε_a^* are the complex permitivity of inner and continuous phase, and are defined by the equations: $\varepsilon_a^* = \varepsilon_a + \kappa_a/(j\omega\varepsilon_o)$, $\varepsilon_i^* = \varepsilon_i + \kappa_i/(j\omega\varepsilon_o)$, respectively. According to Fig. 1, at water content lower than 40% reverse micelles are substantive in the solution, and after 60% normal micelles are predominant. So the W/O and O/W models should be adopted to the systems at lower and higher water content, in which ε_a is equal to 17.10 and 80.00 respectively. However, there is not a model applicable to the B.C. phase at present, therefore, the W/O and O/W models are both applied to calculate the phase parameters of B.C. phase. All phase parameters calculated by Hanai's method are summarized in Table 2 and Table 3.[22] ε_a is equal to permittivity of water (80.00) and that of *n*-butanol (17.10) for O/W model and W/O model respectively in all calculation.

Table 2 Phase parameters in W/O and O/W micelles

	H_2O (%)	$10^4\kappa_a$ (S/m)	$10^2\kappa_i$ (S/m)	$10^2\phi$
W/O Model	15.70	1.99	1.00	87.77
	20.10	3.08	0.95	88.14
	25.80	4.83	1.00	88.40
	30.30	6.41	1.11	88.52
	35.30	8.02	1.13	88.83
O/W Model	70.10	60.98	1.55	81.07
	75.00	58.19	1.41	80.76
	80.00	54.65	1.27	80.19
	95.00	29.43	1.18	79.90

In W/O micellar region, solubilization of water in the palisade layer and inner core of micelles leads to an increase in the size of the micelle, resulting in an increase in the volume fraction of the dispersed phase (micellar particles) with the increase of water content. However, in O/W miceller region, the addition of water reduces the concentration of particles, so ϕ decreases gradually. The volume fraction of the dispersed phase in W/O micelles is larger than that in O/W micelles. In B.C. phase, ϕ only shows the apparent volume fraction of dispersed phase, because the dispersed phase and medium can not be distinguished distinctly. The average value ϕ_a obtained from W/O and O/W models will be considered as the volume fraction of dispersed phase in B.C. region. It can be seen that the volume fraction obtained from O/W model is smaller than that from W/O model. The increase of water content has little effect on the volume fraction ϕ_a in B.C. phase, which is consistent with the previous results discussed.

Varying the n-butanol content

When the weight ratio of SDES/H_2O is fixed at 4:6, ε and κ of systems as functions of frequency with the increase of *n*-butanol content are shown in Fig. 7 (a) and (b). In the frequency range $20-10^4$ Hz, permittivity increases and conductivity decreases gradually with alcohol content, indicating that there exist no essential structural transition in this process, as discussed in Fig. 1.

Table 3 Phase parameters in B.C. phase

O/W Model				W/O Model			
H_2O (%)	$10^3\kappa_a$ (S/m)	$10^2\kappa_i$ (S/m)	$10^2\phi$	$10^3\kappa_a$ (S/m)	$10^2\kappa_i$ (S/m)	$10^2\phi$	$10^2\phi_a$
41.20	4.72	1.05	81.50	1.01	1.17	88.94	85.22
46.00	5.37	1.14	81.58	1.15	1.26	88.98	85.28
49.90	5.84	1.20	81.50	1.25	1.33	88.94	85.22
55.20	6.17	1.57	81.50	1.32	1.72	88.94	85.22
60.20	6.46	1.68	81.30	1.38	1.85	88.82	85.06

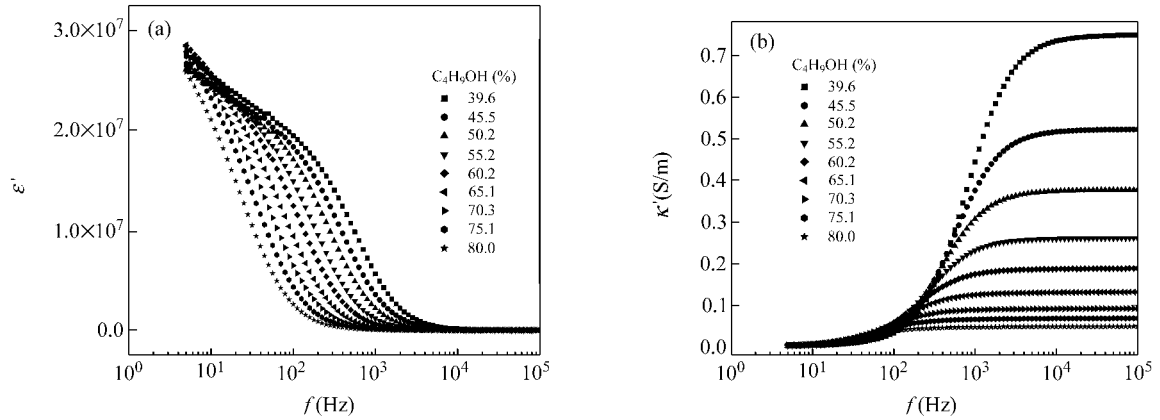

Fig. 7 Permittivity (a) and conductivity (b) as functions of frequency for the systems with different alcohol content.

Dielectric parameter values are also obtained by nonlinear curve fitting as that in Fig. 4. Fig. 8 shows the dielectric relaxation strength, $\Delta\varepsilon$ and $\Delta\kappa$, as functions of alcohol content. $\Delta\varepsilon$ increases and $\Delta\kappa$ decreases gradually with the increment of *n*-butanol content, indicating that there is onefold aggregate in this region, *i.e.*, W/O micelles. τ_0 does likewise, and it increases gradually with the alcohol content, as presented in Fig. 9. Phase parameters are also calculated by Hanai's method and the W/O model was adopted, listed in Table 4. From Table 4, it can be seen that with the increase of *n*-butanol content, the micelle concentration decreases and the water core in the micelle becomes smallar, resulting in the decrease in both κ_a and κ_i.

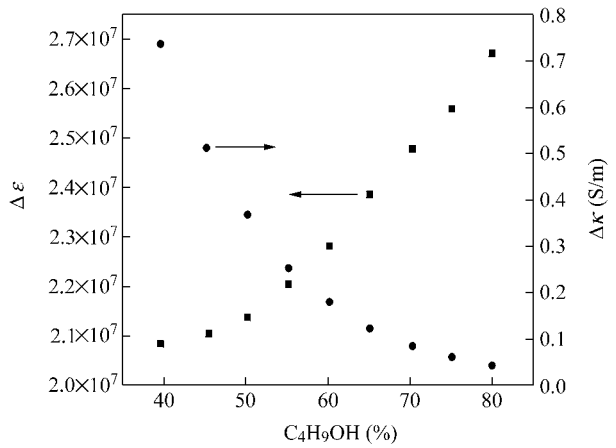

Fig. 8 Relaxation strength, $\Delta\varepsilon$ (■) and $\Delta\kappa$ (●) as functions of alcohol content.

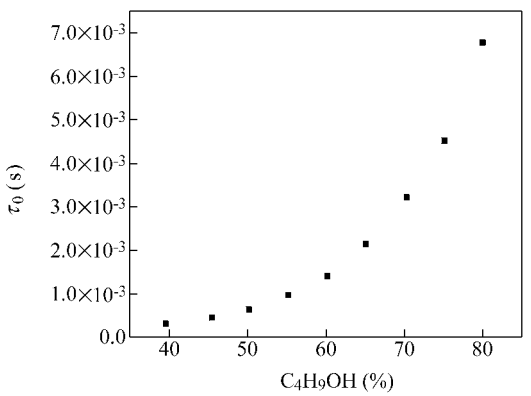

Fig. 9 Characteristic relaxation time τ_0 as a function of alcohol content.

Table 4 Phase parameters in W/O micelles with the increase of *n*-butanol content

C_4H_9OH (%)	$10^4\,\kappa_a$ (S/m)	$10^3\,\kappa_i$ (S/m)	$10^2\,\phi$
39.60	7.54	10.89	89.97
45.50	5.35	8.87	89.91
50.20	3.98	8.48	89.80
55.20	2.87	8.28	89.66
60.20	2.17	8.20	89.47
65.10	1.60	7.84	89.22
70.30	1.32	7.43	88.62
75.10	1.04	7.34	88.33
80.00	0.85	7.53	87.81

According to the previous discussion, τ_0 decreases and the volume fraction of dispersed phase increases in W/O micellar region as water content increases. The alcohol content increases from 39.6% to 80.0%, so the whole system studied belongs to W/O micelles from Fig. 2. Therefore, the concentration of micellar particles and water molecules will become small, which reduces the conductivity of systems, resulting in an increase in τ_0 and a decrease in volume fraction of micellar particles with the increase of alcohol content. The results are in agreement with those obtained in Figs. 5, 6 and Tables 2 and 3.

Conclusions

Phase behavior and dielectric relaxation spectroscopy of the SDES/*n*-C_4H_9OH/H_2O ternary system are investigated by increasing water or alcohol content at a fixed weight ratio of the other two components. Cole-Cole formulae and Hanai's method are applied to fit and calculate dielectric parameters and phase parameters. DRS is the

macro-exhibition of microstructure changes of systems studied. With the increase of water content, characteristic relaxation time decreases in W/O micelles and increases in O/W micelles, and the volume fraction of dispersed phase shows reverse rules. However, in B.C. phase, water content has little effect on the relaxation process and phase parameters. The results obtained by increasing alcohol content in W/O micelles are in agreement with the abovementioned. Dielectric relaxation spectroscopy provides a simple, quick, and reasonable method to indicate the structural transition of surfactant aggregates.

References

1 Bhatnagar, S.; Vyas, S. P. J. *Microencapsulation* **1994**, *11*, 431.
2 Canadas, O.; Valiente, M.; Rodenas, E. *J. Colloid Interface Sci*. **1998**, *203*, 294.
3 Molinero, I.; Sierra, M. L.; Rodenas, E. *J. Colloid Interface Sci*. **1997**, *188*, 239.
4 Montalvo, G.; Valiente, M.; Rodenas, E. *J. Colloid Interface Sci*. **1995**, *172*, 494.
5 Jonstromer, M.; Strey, R. *J. Phys. Chem*. **1992**, *96*, 5993.
6 Hoffmann, H.; Thunig, C.; Valiente, M. *Colloids Surf*. **1992**, *67*, 223.
7 Gjerde, M. I.; Nerdal, W.; Hoiland, H. *Colloid Polym. Sci*. **1998**, *276*, 503.
8 Smith, G.; Duffy, A. P.; Shen, J.; Ollief, C. J. *J. Pharmaceutical Sci*. **1995**, *84*, 1029.
9 Wilcoxon, J. P.; Williamson, R. L.; Baughman, R. *J. Chem. Phys*. **1993**, *98*, 9933.
10 Imai, S.; Shikata, T. *Langmuir* **1999**, *15*, 8388.
11 Shikata, T.; Imai, S. *Langmuir* **1998**, *14*, 6804.
12 Sjoblom, J.; Gestblom, B. *J. Colloid Interface Sci*. **1987**, *115*, 535.
13 Bordi, F.; Cametti, C.; Codastefano, P.; Sciortino, F.; Tartaglia, P.; Rouch, *J. Prog. Colloid Polym. Sci*. **1997**, *105*, 298.
14 Tanaka, R. *J. Colloid Interface Sci*. **1988**, *122*, 220.
15 Jagur-Gradzinski, J.; Frome, R.; Izatt, R. *J. Colloid Interface Sci*. **1985**, *105*, 73.
16 Hill, R. M.; Cooper, J. *J. Colloid Interface Sci*. **1995**, *174*, 24.
17 Cooper, J.; Hill, R. M. *J. Colloid Interface Sci*. **1996**, *180*, 27.
18 Hanai, T.; Zhang, H. Z.; Sekine, K.; Asaka, K.; Asami, A. *Ferroelectrics* **1988**, *86*, 191.
19 Zhang, H. Z.; Sekine, K.; Hanai, T.; Koizumi, N. *Colloid Polym. Sci*. **1984**, *262*, 513.
20 Cole, K. S.; Cole, R. H. *J. Chem. Phys*. **1941**, *9*, 341.
21 Hanai, T. *Kolloid-Z* **1961**, *177*, 57.
22 Hanai, T. *Bull. Inst. Chem. Res., Kyoto Univ*. **1961**, *39*, 341.

(E0212273 PAN, B. F.; LU, Z. S.)